



Free Convection Caputo-Fabrizio Casson Blood Flow in the Cylinder with Slip Velocity

Wan Faezah Wan Azmi¹, Ahmad Qushairi Mohamad^{1,*}, Lim Yeou Jiann¹, Sharidan Shafie¹

¹ Department of Mathematical Sciences, Faculty of Science, Universiti Teknologi Malaysia, 81310 UTM Johor Bahru, Johor, Malaysia

ARTICLE INFO

Article history:

Received 6 September 2022

Received in revised form 8 October 2022

Accepted 12 November 2022

Available online 1 March 2023

Keywords:

Casson Fluid; Caputo-Fabrizio; Slip Velocity; Free Convection; Finite Hankel Transform

ABSTRACT

Recently, fluid with fractional-order derivative model attracted many researchers to further study compared with the classical fluid mode since it is more precise and realistic. To imitate the applications of blood flow in narrow arteries, researchers focused on the fractional Casson fluid flow in the cylinder. However, most researchers solved the problems numerically and without considering the slip effect at the boundary. Thus, obtaining solutions analytically to the unsteady fractional Casson fluid flow in the slip cylinder with free convection is the goal of this study. The Caputo-Fabrizio fractional derivative approach is utilized to model this problem. By joining the approach of the Laplace transform and finite Hankel transform, the fractional governing equations are solved, and analytical solutions to the velocity and temperature profiles are gained. The fluid velocity rises as the slip velocity and Grashof number increase and it declines with the increment of the Casson parameter and Prandtl number. Increasing the fractional parameter will result in an increase in fluid velocity and temperature for a large time interval. The slip velocity effect influenced fluid flow, especially at the cylinder's wall. These findings are beneficial to explore the more fractional-order derivative model and for studying the problems in biomedical engineering.

1. Introduction

Free convection flow is one of the well-known heat transfer processes which is involved with fluid masses, buoyancy force, and gravity force. It happened naturally when there is a temperature difference in a fluid. The hot fluid is less dense than cold fluid which causes hot fluid particles to raise due to the buoyancy force while cold fluid particles go down due to the gravity force. Researchers are attracted to study free convection flow due to its natural and wide applications in engineering such as cooling molten metals, steam pipe and solar ponds, and applications in the medical such as the flow of blood in the small blood vessels with the human temperature [1]. Motivated by it, analytical research on the free convection flow of Newtonian fluid passed through an oscillating cylinder was done by Khan *et al.*, [2]. Javaid *et al.*, [3] solved analytically the similar problem as Ref. [2] by utilizing a different kind of fluid, second-grade fluid, and obtained a similar result. Later, Shah *et al.*, [4] extended the problem by using Maxwell fluid in a fixed cylinder with additional pressure

* Corresponding author.

E-mail address: ahmadqushairi@utm.my (Ahmad Qushairi Mohamad)

gradient and magnetohydrodynamics (MHD) effects. Besides, analytical analysis was done by Abdelhameed [5] to investigate the consequences of free convection flow for Newtonian fluid flowing through an accelerating plate with the MHD effect. They all used the Laplace transform and the Hankel transform to solve problems analytically. They also concluded that a rise in the Grashof number induces a rise in the fluid velocity.

Moreover, fluid consists of liquid or gas are one of the heat carriers which transfer the heat energy from high temperature to low temperature. There are two categories of fluid which are Newtonian fluid and non-Newtonian fluid which is depending on the relationship between strain and stress [6]. The non-Newtonian fluid is against Newton's Law of Viscosity. The common example of a non-Newtonian fluid because of its distinctive behaviour is the Casson fluid. It is a type of yield stress and shear-thinning fluid. When yield stress exceeds applied shear stress, it may act like an elastic solid or no flow may occur while fluid will flow if the condition is inverse. Human blood, juice, honey, jelly, and tomato sauce are a few examples of Casson fluid [7–10]. Inspired by the applications in various fields such as food processing and biotechnology, Mohamad *et al.*, [11] investigated analytically Casson fluid flow past through a fixed channel with a free convection effect. Azmi *et al.*, [12] extended the problem with an additional MHD effect. Then, the analytical solution of the Casson fluid model with free convection flow passed through an exponentially accelerated plate with the effects of MHD and porosity was developed by Ramalingeswara Rao *et al.*, [13]. The Laplace transform method was used to solve each of them analytically. Besides, Ali *et al.*, [14] explored the impact of Casson fluid free convection flow with MHD and pressure gradient effects in an oscillating cylinder. By utilizing the Laplace transform and finite Hankel transform approaches, they were able to obtain analytical solutions. Later, Kumar and Rizvi [15] examined numerically the behavior of free convection flow for the Casson fluid model with the presence of MHD and chemical reaction effects outside the cylinder. They used the Crank-Nicolson implicit finite difference approach to solve numerically. However, these studies lack an introduction fractional derivative model into the governing equations.

Currently, the fractional-derivative fluid model attracted many researchers to expand the studies about it due to the accuracy of the model and the result is more realistic compared to the classical model [16]. L'Hopital and Leibniz initially presented the fractional-order derivative approach concept to discuss the derivative's n -notation in terms of complex, fractional, or irrational numbers. Afterward, several definitions have been established by many researchers to enlighten the usefulness of the fractional derivative model in the applications of fluid mechanics like cooling systems, and biotechnology like cancer cell treatment. Examples of the popular fractional-order derivative are Riemann, Caputo, Riemann-Liouville, Caputo-Fabrizio, and Atangana-Baleanu [17]. Encouraged by its benefits in fluid mechanics applications, Ramzan *et al.*, [18] investigated analytically the influence of the Caputo fractional derivative fluid model on the fluid velocity flow on the inclined plate. They solved by using Laplace transform method. They obtained that increases of fractional parameter led to increase of fluid velocity. Then, Ali *et al.*, [19] obtained analytically the significant difference between the classical model and Caputo fractional model of Casson fluid velocity profiles with MHD effect in the fixed cylinder. Jamil *et al.*, [20,21] investigated an analytically similar problem as [19] in the inclined fixed cylinder and stenosed cylinder. They applied Caputo-Fabrizio fractional derivative model to governing equations. Later, Ali *et al.*, [22] extended the problem by considering the effect of free convection flow in the different boundary conditions such as fixed cylinder, moving cylinder [23], and accelerated cylinder [24]. They compute temperature and velocity profiles analytically by utilizing the Laplace transform and finite Hankel transform techniques. They noticed that as time increases, the fractional model is more realistic than the classical model. However, none of them

investigated the fluid behaviour of the Casson model with the presence of the slip velocity effect in a cylinder.

Velocity gradient occurred between two different mediums known as the slip velocity effect at the cylinder's boundary. It means finite velocity difference between viscous fluid particle movements and boundary-stretching movement [25]. The importance of the slip velocity effect has been highlighted by some researchers such as Nubar [26]. Slip velocity does exist in practical applications like polymer's melting, artificial heart valves and blood flow in blood arteries [27,28]. Padma *et al.*, [29,30] simulate blood flow in stenosed arteries by using the Jeffrey fluid model and taking into account the slip and no-slip effects. They observed that fluid velocity with slip is higher than the no-slip effect. The flow of Casson fluid in the exponentially stretched cylinder with the slip effect was further investigated numerically by Jalil and Iqbal [31]. Additionally, by employing the Casson fluid model, Azmi *et al.*, [32,33] identified analytically the impact of the slip effect at the cylinder's border. By utilizing both Laplace transform and finite Hankel transform methods, they were able to obtain velocity profiles. None of them consider the fractional-order derivatives model in their governing equations.

According to the authors' best knowledge, no researchers had previously addressed analytically the free convection flow of the Casson fluid through a slip boundary of the cylinder by adopting a fractional-order derivative approach. Thus, motivated by it and past studies, the study aims to obtain the analytical solution and evaluate the fractional fluid behaviour of the unsteady free convection flow in the slip velocity cylinder. This study will focus on Casson fluid model since it imitates human blood flow in the small arteries with the slip effect and natural heat transfer process. The momentum and energy governing equations are expressed in the Caputo-Fabrizio fractional derivative model. It consists of a non-singular kernel which is easier to solve the problem compared with the power-law kernel such as Caputo fractional derivative model and therefore it can overcome the limitations in modeling physical problems. Later, a combined Laplace transform together with the finite Hankel transform approach is used to get an analytical solution for velocity and temperature profiles. Then, the obtained analytical solution is plotted and analyzed graphically with the related parameters by using Maple software.

2. Problem Formulation

Since it replicates the human blood flows in the arteries, the investigation of an incompressible Casson fluid flow in a horizontal cylinder with radius r_0 , has been taken into consideration. The z -axis is considered as the direction in which the Casson fluid flows along the cylinder's horizontal axis, while the r -axis is assumed to be normal to it. Casson fluid and the cylinder are at rest with the ambient temperature, T_∞ , at time $t^*=0$. Later, when $t^*>0$, the fluid begins to flow because of a slip velocity. Simultaneously, the temperature of the cylinder is raised from ambient temperature to the wall temperature, T_w and later it remains constant. The physical diagram for the Casson fluid flow issue is shown in Figure 1.

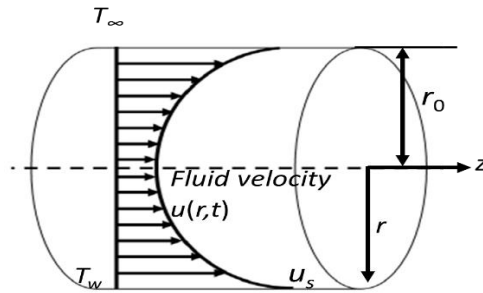


Fig. 1. The physical geometry of the fluid flow

Only r and t constitute the temperature and velocity functions. Additionally, all fluid parameters are considered to be constant, excluding the density of the buoyancy term, which is computed by using Boussinesq's approximation. Given these presumptions, the related partial differential equation for momentum and energy is used to define the problem of unsteady Casson fluid flow in the cylinder as follows [34]

$$\rho \frac{\partial u^*}{\partial t^*} = \mu \left(1 + \frac{1}{\beta} \right) \left(\frac{\partial^2 u^*}{\partial r^{*2}} + \frac{1}{r^*} \frac{\partial u^*}{\partial r^*} \right) + g \rho \beta_T (T^* - T_\infty), \quad (1)$$

and

$$\rho c_p \frac{\partial T^*}{\partial t^*} = k \left(\frac{\partial^2 T^*}{\partial r^{*2}} + \frac{1}{r^*} \frac{\partial T^*}{\partial r^*} \right), \quad (2)$$

together with the related initial and boundary conditions [19,22]

$$\begin{aligned} u^*(r^*, 0) &= 0 & T^*(r^*, 0) &= T_\infty & ; r \in [0, r_0], \\ u^*(r_0^*, t^*) &= u_s & T^*(r_0^*, t^*) &= T_w & ; t^* > 0. \end{aligned} \quad (3)$$

where ρ is the fluid's density, u^* is the velocity component along the z -axis, μ is the fluid's dynamic viscosity, β is the non-Newtonian Casson parameter, g is the gravitational acceleration, β_T is the thermal expansion coefficient, T^* is the fluid's temperature, c_p is the fluids specific heat capacity at constant temperature and k is thermal conductivity. The dimensionless variables [19,22] are presented as

$$t = \frac{t^* V}{r_0^2}, \quad r = \frac{r^*}{r_0}, \quad u = \frac{u^*}{u_0}, \quad u_s = \frac{u_s^*}{u_0}, \quad \theta = \frac{T - T_\infty}{T_w - T_\infty}. \quad (4)$$

By utilizing dimensionless variables Eq. (4) the momentum governing Eq. (1) and the energy governing Eq. (2) are transformed into the dimensionless form together with the initial and boundary conditions in Eq. (3), which obtain as

$$\frac{\partial u}{\partial t} = \beta_1 \left(\frac{\partial^2 u}{\partial r^2} + \frac{1}{r} \frac{\partial u}{\partial r} \right) + Gr \theta \quad (5)$$

$$\frac{\partial \theta}{\partial t} = \frac{1}{\text{Pr}} \left(\frac{\partial^2 \theta}{\partial r^2} + \frac{1}{r} \frac{\partial \theta}{\partial r} \right) \quad (6)$$

together with the appropriate initial and boundary conditions

$$\begin{aligned} u(r, 0) &= 0, & \theta(r, 0) &= 0 & ; r \in [0, 1], \\ u(1, t) &= u_s, & \theta(1, t) &= 1 & ; t > 0 \end{aligned} \quad (7)$$

which $\text{Pr} = \frac{\mu c_p}{k}$ is the Prandtl number and $Gr = \frac{g \beta_T (T_w - T_\infty) r_0^2}{\nu u_0}$ is the Grashof number are the obtained dimensionless parameters. Meanwhile, $\beta_1 = \frac{1}{\beta_0}$ and $\beta_0 = 1 + \frac{1}{\beta}$ are the constant parameters. Then, the dimensionless momentum governing Eq. (5) and dimensionless energy governing Eq. (6) are transformed into Caputo-Fabrizio fractional derivative model which yields

$${}^{CF} D_t^\alpha u(r, t) = \beta_1 \left(\frac{\partial^2 u}{\partial r^2} + \frac{1}{r} \frac{\partial u}{\partial r} \right) + Gr \theta \quad (8)$$

$${}^{CF} D_t^\alpha \theta(r, t) = \frac{1}{\text{Pr}} \left(\frac{\partial^2 \theta}{\partial r^2} + \frac{1}{r} \frac{\partial \theta}{\partial r} \right) \quad (9)$$

where ${}^{CF} D_t^\alpha f(r, t) = \frac{1}{1-\alpha} \int_0^t \exp\left(\frac{-\alpha(\tau-t)}{1-\alpha}\right) f'(\tau) dt$ for $0 < \alpha < 1$ is the definition of the Caputo-Fabrizio fractional derivative [35].

3. Problem Solution

Analytical solutions for the velocity and temperature profiles are formed by joining the Laplace transform and finite Hankel transform. The method for resolving the initial-boundary value and transient problems is the Laplace transform while the finite Hankel transform is useful when dealing with the cylindrical domain.

3.1 Calculation of Temperature

Firstly, Eq. (9), along with the corresponding initial and boundary conditions in Eq. (7), are transformed by using the Laplace transform method, which yields

$$\frac{a_0 s \bar{\theta}(r, s)}{s + a_1} = \frac{1}{\text{Pr}} \left[\frac{\partial^2 \bar{\theta}(r, s)}{\partial r^2} + \frac{1}{r} \frac{\partial \bar{\theta}(r, s)}{\partial r} \right], \quad (10)$$

$$\bar{\theta}(1, s) = \frac{1}{s}, \quad (11)$$

where $a_0 = 1/1 - \alpha$, and $a_1 = a_0\alpha$, are the fractional constant parameters, $\bar{\theta}(r, s)$ is the Laplace transform of the function $\theta(r, t)$ and s is the transformation variable. Secondly, finite Hankel transform of zero-order is applied to the Eq. (10) and by using condition in Eq. (11), give

$$\bar{\theta}_H(r_n, s) = \frac{r_n J_1(r_n)}{s} \left[\frac{s + a_1}{(a_0 \text{Pr} + r_n^2)s + a_1 r_n^2} \right], \tag{12}$$

where $\bar{\theta}_H(r_n, s) = \int_0^1 r \bar{\theta}(r, s) J_0(rr_n) dr$ is the finite Hankel transform of the function $\bar{\theta}(r, s)$ and r_n with $n=0, 1, \dots$ are the positive roots of the equation $J_0(x) = 0$, where J_0 is the Bessel function of the first kind and zero-order, J_1 is the Bessel function of the first kind and first order. Then, Eq. (12) is simplified and obtained as

$$\bar{\theta}_H(r_n, s) = \frac{J_1(r_n)}{r_n} \left[\frac{1}{s} - \frac{a_0 \text{Pr}}{((s + a_3[n])(a_0 \text{Pr} + r_n^2))} \right], \tag{13}$$

where $a_3[n] = a_1 r_n^2 / (a_0 \text{Pr} + r_n^2)$ is the constant parameter. Thirdly, the inverse Laplace transform is applied to the Eq. (13) gaining as

$$\theta_H(r_n, t) = \frac{J_1(r_n)}{r_n} \left[1 - \frac{a_0 \text{Pr} \exp(-a_3[n]t)}{a_0 \text{Pr} + r_n^2} \right]. \tag{14}$$

Lastly, to solve the equation analytically for temperature profile in Eq. (14), the inverse finite Hankel transform is being used and attained as

$$\theta(r, t) = 1 - 2a_0 \text{Pr} \sum_{n=1}^{\infty} \frac{J_0(rr_n) \exp(-a_3[n]t)}{r_n J_1(r_n) (a_0 \text{Pr} + r_n^2)}. \tag{15}$$

3.2 Calculation of Velocity

The Laplace transform is employed in Eq. (8) together with the related initial and boundary conditions in Eq. (7), which yields

$$\frac{a_0 s \bar{u}(r, s)}{s + a_1} = \beta_1 \left[\frac{\partial^2 \bar{u}(r, s)}{\partial r^2} + \frac{1}{r} \frac{\partial \bar{u}(r, s)}{\partial r} \right] + Gr \bar{\theta}(r, s), \tag{16}$$

$$\bar{u}(1, s) = \frac{u_s}{s}, \tag{17}$$

where $\bar{u}(r, s)$ is the Laplace transform of the function $u(r, t)$. Next, Laplace's partial differential Eq. (16) together with the boundary conditions in Eq. (17) is used in the method of finite Hankel transform of zero-order to transform into an ordinary differential equation (ODE), giving

$$\bar{u}_H(r_n, s) = \left(\beta_1 r_n J_1(r_n) \frac{u_s}{s} + Gr \bar{\theta}_H(r_n, s) \right) \left(\frac{s + a_1}{(a_0 + \beta_1 r_n^2) s + a_1 \beta_1 r_n^2} \right), \quad (18)$$

where $\bar{u}_H(r_n, s) = \int_0^1 r \bar{u}(r, s) J_0(r r_n) dr$ is the finite Hankel transform of the function $\bar{u}(r, s)$. Eq. (19) can be written in an appropriate form as

$$\bar{u}_H(r_n, s) = F_1(s) + F_2(s) - F_3(s), \quad (19)$$

with

$$F_1(s) = \frac{J_1(r_n)}{r_n} \left[\frac{u_s}{s} - \frac{a_0 u_s}{\left(s + \frac{a_4[n]}{a_5[n]} \right) a_5[n]} \right], \quad F_2(s) = \frac{J_1(r_n)}{r_n} \frac{Gr}{\beta_1 r_n^2} \left[\frac{1}{s} - \frac{a_0}{a_5[n] \left(s + \frac{a_4[n]}{a_5[n]} \right)} \right],$$

$$F_3(s) = \frac{J_1(r_n)}{r_n^3} \frac{Gra_0 Pr}{(\beta_1 Pr - 1)} \left[\frac{Pr}{(a_0 Pr + r_n^2)(s + a_3[n])} - \frac{1}{a_5[n] \left(s + \frac{a_4[n]}{a_5[n]} \right)} \right].$$

where $a_4[n] = a_1 \beta_1 r_n^2$, and $a_5[n] = a_0 + \beta_1 r_n^2$ are the constant parameters. Then, the inverse Laplace transform is applied to Eq. (20), which can be obtained as

$$u_H(r_n, t) = f_1(t) + f_2(t) - f_3(t), \quad (20)$$

With

$$f_1(t) = \frac{J_1(r_n)}{r_n} \left(u_s - \frac{a_0 u_s}{a_5[n]} \exp\left(-\frac{a_4[n]}{a_5[n]} t\right) \right), \quad f_2(t) = \frac{J_1(r_n)}{r_n} \frac{Gr}{\beta_1 r_n^2} \left[1 - \frac{a_0}{a_5[n]} \exp\left(-\frac{a_4[n]}{a_5[n]} t\right) \right],$$

$$f_3(t) = \frac{J_1(r_n)}{r_n^3} \frac{Gra_0 Pr}{(\beta_1 Pr - 1)} \left[\frac{Pr}{a_0 Pr + r_n^2} \exp(-a_3[n]t) - \frac{1}{a_5[n]} \exp\left(-\frac{a_4[n]}{a_5[n]} t\right) \right].$$

The analytical solution for velocity profiles is then solved by applying the inverse finite Hankel transform to the Eq. (21) which is written as

$$\begin{aligned}
 u(r,t) = & u_s - 2a_0u_s \sum_{n=1}^{\infty} \frac{J_0(rr_n)}{r_n J_1(r_n)} \frac{1}{a_5[n]} \exp\left(-\frac{a_4[n]}{a_5[n]}t\right) \\
 & + \frac{2Gr}{\beta_1 \text{Pr} - 1} \sum_{n=1}^{\infty} \frac{J_0(rr_n)}{r_n^3 J_1(r_n)} \left[\begin{aligned} & \frac{\beta_1 \text{Pr} - 1}{\beta_1} + \frac{a_0}{a_5[n]\beta_1} \exp\left(-\frac{a_4[n]}{a_5[n]}t\right) \\ & - \frac{a_0 \text{Pr}^2}{a_0 \text{Pr} + r_n^2} \exp(-a_3[n]t) \end{aligned} \right]. \tag{21}
 \end{aligned}$$

4. Result and Discussion

The blood flow characteristics with the fractional derivative model had been analyzed and plotted graphically with the involved important parameters including Casson parameter β , Grashof number Gr , Prandtl number Pr , slip velocity parameter u_s , fractional parameter α , and time parameter t . The limiting case of the solved analytical solution (21) is compared with the earlier result by Khan *et al.*, [2] to verify the accuracy of the solution. This comparison is shown in Figure 2. Based on the observation, both graphs are aligned which indicates both graphs are in mutual agreement. Hence, the analytical result that was obtained is accepted.

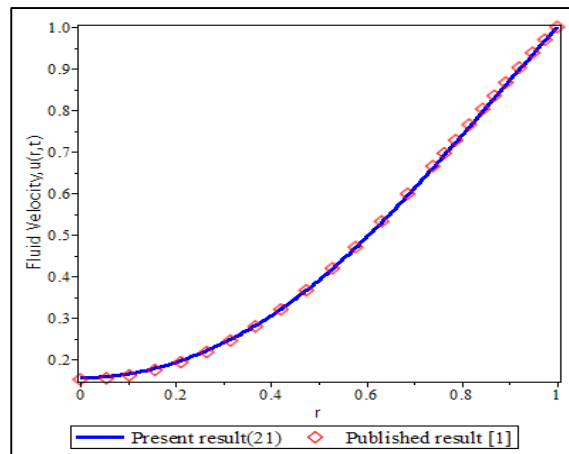


Fig. 2. Comparison of velocity profile $u(r,t)$ from Eq. (21) when $\beta \rightarrow \infty$, $u_s=1.0$, $\alpha=0.999$ with Eq. (21) when $\omega=0$ by Khan *et al.*, [1].

Figure 3 to Figure 9 illustrate the visual discussion on the impacts of related parameters like slip velocity parameter u_s , Casson parameter β , fractional parameter α , Grashof number Gr , Prandtl number Pr and time parameter t for the fluid velocity $u(r,t)$ and fluid temperature $\vartheta(r,t)$ versus radial coordinate r . The next parametric values are specified for numerical computation based on the physical values provided in Refs. [2,23,29,35]: $u_s=0.1$ for slip condition, $u_s=0$ for no-slip condition, $Pr=21.0$ Prandtl number for blood, $t=0.4$ for initial state condition, $t=3.0$ for steady state condition, $\beta=0.8$, $Gr=1.0$, $\alpha=0.5$, and the estimated ranges of significant parameters values are as follows: $\beta=0.4,0.8,1.2$, $Pr=5.0,7.2,21$. Besides, in order to obtain broad spectrum plotted graph of the findings, some of the range parameters are approximated as: $Gr=0.5,1.0,1.5$, $\alpha=0.3,0.5,0.7$ and $t=0.1,1.0$.

The Casson parameter β impacts the Casson fluid velocity behaviour with the existence of the slip and no-slip boundary display in Figure 3. Generally, the behaviour of Casson fluid which imitates human blood flow in the small arteries can be seen as a Casson parameter close to zero [35]. According to the graph's observation, a higher Casson parameter will result in a slower fluid flow. It

is due to the increase of the internal friction and shear thickening factor of the fluid. Thus, the fluid thickens and becomes more viscous, leading to the fluid's velocity reduction.

Figure 4 illustrates the thermal Grashof number Gr impact on fluid velocity. The figure consists of the graphs with the no-slip and slip velocity effect at the cylinder's wall. This demonstrates the rise of fluid velocity as the thermal Grashof number increases. It is because the thermal buoyancy force will increase as Gr increases. In the case of a free convection flow, the buoyancy force is predominant. As fluid temperature rises, the viscous force impact is lessened by the buoyant force that results from a decrease in fluid density. Consequently, it enhances fluid velocity.

Meanwhile, fluid velocity and fluid temperature decrease with increases in Prandtl number Pr as illustrated in Figure 5 and Figure 6. The fluid behaviour with the same decrement pattern for the slip and no-slip velocity effect is shown in Figure 5. Increasing Pr will increase the momentum diffusivity and viscous force of the fluid while decreasing the thermal diffusivity. The thermal diffusivity is thus dominated by viscous force, which also increases the resistance of fluid motion. Thereby, velocity and temperature profiles will decrease as the Prandtl number increase. Besides that, temperature profiles increase as the time parameter increases.

Figure 7 shows the fluid velocity behaviour as the slip velocity, u_s , and time, t change. The increment value of the slip velocity and time parameter is found to increase fluid velocity. It is obviously can be seen on the wall of the cylinder, $r=1$. It is due to the velocity gradient that exists between two different mediums which are the solid boundary cylinder and fluid particles that flow through the cylinder. Therefore, fluid velocity at $r=1$ will be equal to the slip velocity occurring at the cylinder's boundary and increase as it approaches the center of the cylinder at $r=0$ for a longer period. Meanwhile, fluid velocity decrease as an approach to $r=0$ when the slip velocity increase for a smaller time interval. It is due to the viscous force being high when an approach to $r=0$ since the heat transfer process is not equally distributed in the fluid.

Finally, Figure 8 and Figure 9 show how fractional parameters affect fluid temperature and velocity. It is discovered that fluid temperature and velocity fall over a shorter period ($t=0.4$) when fractional parameters rise. Meanwhile, fluid velocity and fluid temperature increase as fractional parameters increase for a larger time interval $t=3.0$. It demonstrates that the fractional parameter is a significant factor in regulating the fluid's flow velocity and temperature. Since fractional derivatives have memory effects, there are differences between small time and large periods. Therefore, as time increases, fluid behaviour from an unsteady state will achieve the steady-state condition which means that the fluid system is stable.

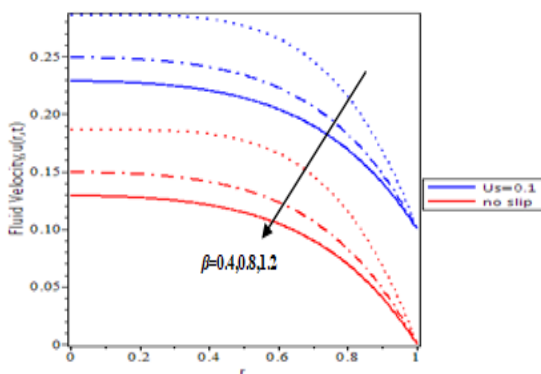


Fig. 3. Casson parameter impact on fluid velocity behaviour $u(r,t)$ when $\alpha=0.5$, $Gr=1$, $Pr=21$ and $t=3$

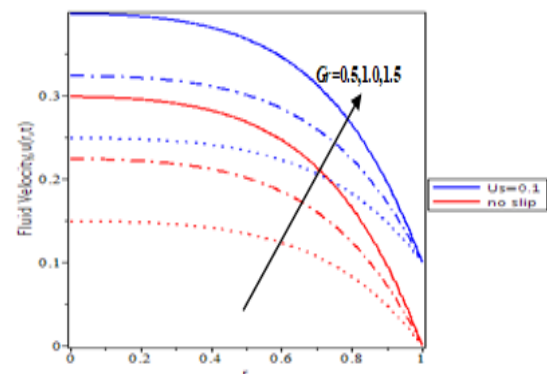


Fig. 4. Thermal Grashof number impact on fluid velocity behaviour $u(r,t)$ when $\alpha=0.5$, $\beta=0.8$, $Pr=21$ and $t=3$

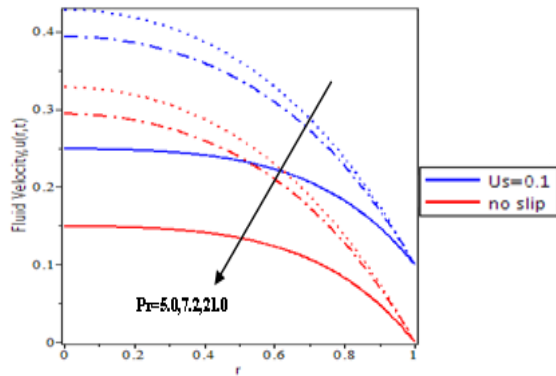


Fig. 5. Prandtl number impact on fluid velocity behaviour $u(r,t)$ when $\alpha=0.5$, $\beta=0.8$, $Gr=1.0$ and $t=3$

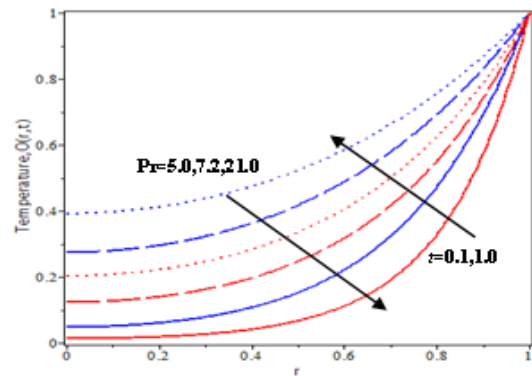


Fig. 6. Prandtl number and time impact on fluid temperature behaviour $\vartheta(r,t)$ when $\alpha=0.5$

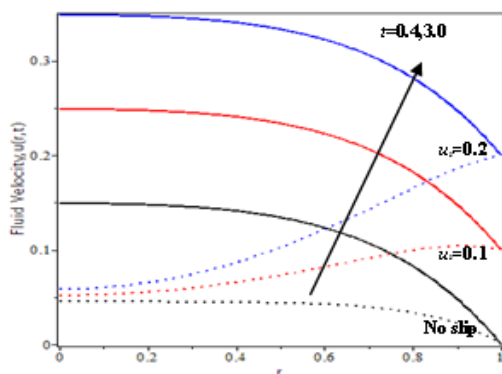


Fig. 7. Slip velocity and time impact on fluid velocity behaviour $u(r,t)$ when $\alpha=0.5$, $\beta=0.8$, $Gr=1.0$ and $Pr=21$

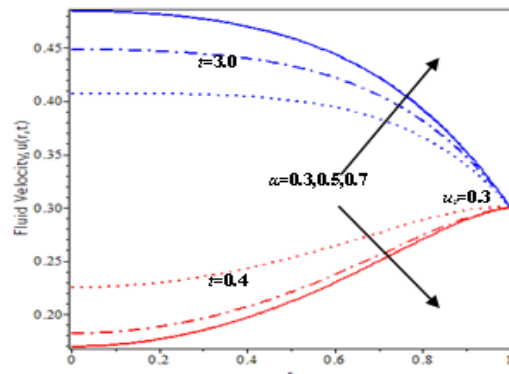


Fig. 8. Fractional parameter impact on fluid velocity behaviour $u(r,t)$ when $\beta=0.8$, $u_s=0.3$, $Gr=1.0$ and $Pr=21$

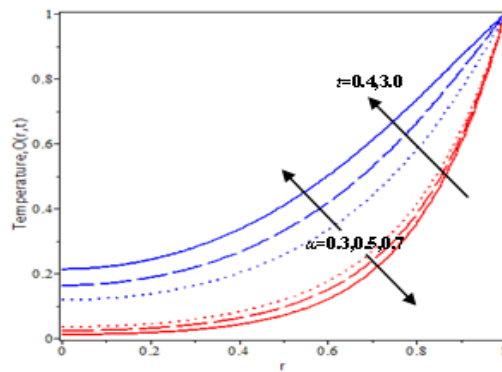


Fig. 9. Fractional parameter and time impact on the temperature of fluid behaviour $\vartheta(r,t)$ when $Pr=21.0$

5. Conclusion

The present study obtained analytical solutions of the fractional Casson fluid model with the free convection flow and the slip velocity effect passed through a cylinder. To gain solutions of velocity and temperature profiles analytically, the Laplace transform together with the finite Hankel transform are employed together. The obtained findings are very useful to study the human blood flow in the small arteries. The results lead to the conclusion that;

- i. Fractional parameter increases will enhance fluid velocity and temperature for a larger time interval and vice versa.
- ii. The fluid velocity at the cylinder wall is significantly impacted by slip velocity.
- iii. The obtained analytical solution is identical to the previously published result. The obtained solution is accepted.
- iv. Increases in u_s , Gr , and t lead to fluid velocity enhancement.
- v. Increasing values of β and Pr cause decreasing values of fluid velocity.
- vi. Fluid temperature increases as Pr decreases and t increases.

This study can be extended for future research by including additional effects of MHD, porous media, radiation, and chemical reaction as well as other types of fluid. Other than that, the advanced contribution can be focused on nanofluids and hybrid nanofluids.

Acknowledgement

The authors would like to acknowledge the Ministry of Higher Education Malaysia and Research Management Centre-UTM, University Technology Malaysia (UTM) for financial support through vote numbers 4B748 and 03M77.

References

- [1] Zokri, Syazwani Mohd, Nur Syamilah Arifin, Abdul Rahman Mohd Kasim, and Mohd Zuki Salleh. "Free convection boundary layer flow of Jeffrey nanofluid on a horizontal circular cylinder with viscous dissipation effect." *Journal of Advanced Research in Micro and Nano Engineering* 1, no. 1 (2020): 1-14.
- [2] Khan, Ilyas, Nehad Ali Shah, Asifa Tassaddiq, Norzieha Mustapha, and Seripah Awang Kechil. "Natural convection heat transfer in an oscillating vertical cylinder." *PLoS one* 13, no. 1 (2018): e0188656. <https://doi.org/10.1371/journal.pone.0188656>
- [3] Javaid, Maria, M. Imran, M. A. Imran, I. Khan, and K. S. Nisar. "Natural convection flow of a second grade fluid in an infinite vertical cylinder." *Scientific Reports* 10, no. 1 (2020): 1-11. <https://doi.org/10.1038/s41598-020-64533-z>
- [4] Shah, Nehad Ali, Aziz Ullah Awan, Rabia Khan, Iskander Tlili, M. Umar Farooq, Bashir Salah, and Jae Dong Chung. "Free convection Hartmann flow of a viscous fluid with damped thermal transport through a cylindrical tube." *Chinese Journal of Physics* (2022). <https://doi.org/10.1016/j.cjph.2020.09.032>
- [5] Abdelhameed, Tarek N. "Entropy generation analysis for MHD flow of water past an accelerated plate." *Scientific Reports* 11, no. 1 (2021): 1-11. <https://doi.org/10.1038/s41598-021-89744-w>
- [6] Thirupathi, Gurralla, Kamatam Govardhan, and Ganji Narendar. "Radiative Magnetohydrodynamics Casson Nanofluid Flow and Heat and Mass Transfer past on Nonlinear Stretching Surface." *Journal of Advanced Research in Numerical Heat Transfer* 6, no. 1 (2021): 1-21.
- [7] Alderman, N. J. "Non-Newtonian fluids: guide to classification and characteristics." *London: ESDU* (1997).
- [8] Chhabra, Rajendra P. "Non-Newtonian fluids: an introduction." In *Rheology of complex fluids*, pp. 3-34. Springer, New York, NY, 2010. https://doi.org/10.1007/978-1-4419-6494-6_1
- [9] Yusof, Nur Syamila, Siti Khuzaimah Soid, Mohd Rijal Illias, Ahmad Sukri Abd Aziz, and Nor Ain Azeany Mohd Nasir. "Radiative Boundary Layer Flow of Casson Fluid Over an Exponentially Permeable Slippery Riga Plate with Viscous Dissipation." *Journal of Advanced Research in Applied Sciences and Engineering Technology* 21, no. 1 (2020): 41-51. <https://doi.org/10.37934/araset.21.1.4151>
- [10] Mohamed, Muhammad Khairul Anuar, Siti Hanani Mat Yasin, and Mohd Zuki Salleh. "Slip Effects on MHD Boundary Layer Flow over a Flat Plate in Casson Ferrofluid." *Journal of Advanced Research in Fluid Mechanics and Thermal Sciences* 88, no. 1 (2021): 49-57. <https://doi.org/10.37934/arfm.88.1.4957>
- [11] Qushairi, Mohamad Ahmad, Jiann Lim Yeou, Sharidan Shafie, Ilyas Khan, and Zulkhibri Ismail. "Exact solution for unsteady free convection flow of Casson fluid in vertical channel." In *MATEC Web of Conferences*, vol. 189, p. 01007. EDP Sciences, 2018. <https://doi.org/10.1051/mateconf/201818901007>
- [12] Azmi, Wan Faezah Wan, Ahmad Qushairi Mohamad, Yeak Su Hoe, Zaiton Mat Isa, and Sharidan Shafie. "Effects of Magnetohydrodynamics and Heat Transfer in Casson Fluid Through a Channel." *Malaysian Journal of Fundamental and Applied Sciences* 17, no. 4 (2021): 416-429. <https://doi.org/10.11113/mjfas.v17n4.2068>
- [13] Rao, S. Ramalingeswara, G. Vidyasagar, and G. V. S. R. Deekshitulu. "Unsteady MHD free convection Casson fluid flow past an exponentially accelerated infinite vertical porous plate through porous medium in the presence of

- radiation absorption with heat generation/absorption." *Materials Today: Proceedings* 42 (2021): 1608-1616. <https://doi.org/10.1016/j.matpr.2020.07.554>
- [14] Ali, Farhad, Salman Yousaf, Ilyas Khan, and Nadeem Ahmad Sheikh. "A new idea of Atangana-Baleanu time fractional derivatives to blood flow with magnetic particles in a circular cylinder: two phase flow model." *Journal of Magnetism and Magnetic Materials* 486 (2019): 165282. <https://doi.org/10.1016/j.jmmm.2019.165282>
- [15] Kumar, Gaurav, and S. M. K. Rizvi. "Casson fluid flow past on vertical cylinder in the presence of chemical reaction and magnetic field." *Applications and Applied Mathematics: An International Journal (AAM)* 16, no. 1 (2021): 28.
- [16] Shaikh, Amjad, Asifa Tassaddiq, Kottakkaran Sooppy Nisar, and Dumitru Baleanu. "Analysis of differential equations involving Caputo–Fabrizio fractional operator and its applications to reaction–diffusion equations." *Advances in Difference Equations* 2019, no. 1 (2019): 1-14. <https://doi.org/10.1186/s13662-019-2115-3>
- [17] Ross, Bertram. "A brief history and exposition of the fundamental theory of fractional calculus." *Fractional calculus and its applications* (1975): 1-36. <https://doi.org/10.1007/BFb0067096>
- [18] Ramzan, Muhammad, Zaib Un Nisa, Ahmad Shafique, and Mudassar Nazar. "Slip and Thermo Diffusion Effects on the Flow Over an Inclined Plate." *Journal of Advanced Research in Fluid Mechanics and Thermal Sciences* 94, no. 2 (2022): 13-28. <https://doi.org/10.37934/arfmts.94.2.1328>
- [19] Ali, Farhad, Nadeem Ahmad Sheikh, Ilyas Khan, and Muhammad Saqib. "Magnetic field effect on blood flow of Casson fluid in axisymmetric cylindrical tube: A fractional model." *Journal of Magnetism and Magnetic Materials* 423 (2017): 327-336. <https://doi.org/10.1016/j.jmmm.2016.09.125>
- [20] Jamil, Dzuliana Fatin, Salah Uddin, M. Ghazali Kamardan, and Rozaini Roslan. "The effects of magnetic blood flow in an inclined cylindrical tube using caputo-fabrizio fractional derivatives." *CFD Letters* 12, no. 1 (2020): 111-122.
- [21] Jamil, Dzuliana Fatin, Salman Saleem, Rozaini Roslan, Fahad S. Al-Mubaddel, Mohammad Rahimi-Gorji, Alibek Issakhov, and Salah Ud Din. "Analysis of non-Newtonian magnetic Casson blood flow in an inclined stenosed artery using Caputo–Fabrizio fractional derivatives." *Computer Methods and Programs in Biomedicine* 203 (2021): 106044. <https://doi.org/10.1016/j.cmpb.2021.106044>
- [22] Ali, Farhad, Anees Imtiaz, Ilyas Khan, and Nadeem Ahmad Sheikh. "Flow of magnetic particles in blood with isothermal heating: A fractional model for two-phase flow." *Journal of Magnetism and Magnetic Materials* 456 (2018): 413-422. <https://doi.org/10.1016/j.jmmm.2018.02.063>
- [23] Ali, Farhad, Anees Imtiaz, Ilyas Khan, Nadeem Ahmad Sheikh, and Dennis Ling Chuan Ching. "Hemodynamic flow in a vertical cylinder with heat transfer: two-phase Caputo Fabrizio fractional model." *Journal of Magnetism* 23, no. 2 (2018): 179-191. <https://doi.org/10.4283/JMAG.2018.23.2.179>
- [24] Ali, Farhad, Nabeel Khan, Anees Imtiaz, Ilyas Khan, and Nadeem Ahmad Sheikh. "The impact of magnetohydrodynamics and heat transfer on the unsteady flow of Casson fluid in an oscillating cylinder via integral transform: A Caputo–Fabrizio fractional model." *Pramana* 93, no. 3 (2019): 1-12. <https://doi.org/10.1007/s12043-019-1805-4>
- [25] Rao, I. J., and K. R. Rajagopal. "The effect of the slip boundary condition on the flow of fluids in a channel." *Acta Mechanica* 135, no. 3 (1999): 113-126. <https://doi.org/10.1007/BF01305747>
- [26] Nubar, Yves. "Blood flow, slip, and viscometry." *Biophysical Journal* 11, no. 3 (1971): 252-264. [https://doi.org/10.1016/S0006-3495\(71\)86212-4](https://doi.org/10.1016/S0006-3495(71)86212-4)
- [27] Rozeli, Nurliyana Syamira, Ahmad Nazri Mohd Som, Norihan Md Arifin, Fadzilah Md Ali, and Aniza Abd Ghani. "Double Stratified MHD Stagnation Point Slip Flow Over a Permeable Shrinking/Stretching Surface in A Porous Medium." *Journal of Advanced Research in Fluid Mechanics and Thermal Sciences* 90, no. 2 (2022): 64-72. <https://doi.org/10.37934/arfmts.90.2.6472>
- [28] Noor, Nur Azlina Mat, Mohd Ariff Admon, and Sharidan Shafie. "Unsteady MHD Squeezing Flow of Casson Fluid Over Horizontal Channel in Presence of Chemical Reaction." *Journal of Advanced Research in Fluid Mechanics and Thermal Sciences* 92, no. 2 (2022): 49-60. <https://doi.org/10.37934/arfmts.92.2.4960>
- [29] Padma, R., R. Tamil Selvi, and R. Ponalagusamy. "Effects of slip and magnetic field on the pulsatile flow of a Jeffrey fluid with magnetic nanoparticles in a stenosed artery." *The European Physical Journal Plus* 134, no. 5 (2019): 221. <https://doi.org/10.1140/epjp/i2019-12538-9>
- [30] Padma, R., R. Ponalagusamy, and R. Tamil Selvi. "Mathematical modeling of electro hydrodynamic non-Newtonian fluid flow through tapered arterial stenosis with periodic body acceleration and applied magnetic field." *Applied Mathematics and Computation* 362 (2019): 124453. <https://doi.org/10.1016/j.amc.2019.05.024>
- [31] Jalil, M., and W. Iqbal. "Numerical analysis of suction and blowing effect on boundary layer slip flow of Casson fluid along with permeable exponentially stretching cylinder." *AIP Advances* 11, no. 3 (2021): 035304. <https://doi.org/10.1063/5.0042314>
- [32] Azmi, Wan Faezah Wan, Ahmad Qushairi Mohamad, Lim Yeou Jiann, and Sharidan Shafie. "Analytical Solution of Unsteady Casson Fluid Flow Through a Vertical Cylinder with Slip Velocity Effect." *Journal of Advanced Research in Fluid Mechanics and Thermal Sciences* 87, no. 1 (2021): 68-75. <https://doi.org/10.37934/arfmts.87.1.6875>

- [33] Azmi, Wan Faezah Wan, Ahmad Qushairi Mohamad, Lim Yeou Jiann, and Sharidan Shafie. "UNSTEADY MHD CASSON FLUID FLOW IN A VERTICAL CYLINDER WITH POROSITY AND SLIP VELOCITY EFFECTS." In *e-Proceedings of the 5 th International Conference on Computing, Mathematics and Statistics (iCMS 2021)*, p. 60. 2021. <https://doi.org/10.37934/arfmts.87.1.6875>
- [34] Maiti, Subrata, Sachin Shaw, and G. C. Shit. "Fractional order model for thermochemical flow of blood with Dufour and Soret effects under magnetic and vibration environment." *Colloids and Surfaces B: Biointerfaces* 197 (2021): 111395. <https://doi.org/10.1016/j.colsurfb.2020.111395>
- [35] Maiti, S., S. Shaw, and G. C. Shit. "Caputo–Fabrizio fractional order model on MHD blood flow with heat and mass transfer through a porous vessel in the presence of thermal radiation." *Physica A: Statistical Mechanics and its Applications* 540 (2020): 123149. <https://doi.org/10.1016/j.physa.2019.123149>